2021

Modeling of the NIST Intelligent Building Agents Labratory

Adam Jacob Kopach
University of Wisconsin-Madison, United States of America, akopach@wisc.edu

Modelling the NIST IBAL

Adam KOPACH[1]*, Greg NELLIS[2], David BRADLEY[3], Doug REINDL[4], Amanda PERTZBORN[5]

[1]University of Wisconsin, Department of Mechanical Engineering,
Madison, WI, United States
akopach@wisc.edu

[2]University of Wisconsin, Department of Mechanical Engineering,
Madison, WI, United States
gfnellis@engr.wisc.edu

[4]Thermal Energy System Specialists, Principal Investigator
Madison, WI, United States
d.bradley@tess-inc.com

[3]University of Wisconsin, Department of Mechanical Engineering,
Madison, WI, United States
dreindl@wisc.edu

[5]NIST, Engineering Laboratory
Gaithersburg, MD, United States
amanda.pertzborn@nist.gov

* Corresponding Author

ABSTRACT

The Intelligent Building Agents Laboratory (IBAL) at the National Institute of Standards and Technology (NIST) will be used to experimentally study control strategies within the realm of commercial building air-conditioning systems. A simulation software (Klein, 2020) model of the IBAL has been created to help guide the experiments in the IBAL and to provide a software-based method of evaluating control strategies implemented in this facility. This simulation model is composed of the various components comprising the IBAL HVAC system such as heating coils, cooling coils, fans and dampers that can accurately simulate the actual component behavior under transient and off-design conditions. Additionally, pressure and airflow throughout the system are simulated to support associated controls for modulating damper positions and fan speeds. The resulting system simulation is flexible; it is possible to study the expected IBAL system response to forcing functions such as weather and loads under the influence of different control strategies. The initial controller included in the IBAL simulation model replicates the controls used in most commercial buildings. The resulting tool will be validated in the IBAL and allow NIST to test alternate, advanced control strategies quickly, providing guidance for the experimental work.

1. INTRODUCTION

According to the U.S. Energy Information Administration, the commercial buildings sector consumed over 106 quadrillion kJ, or roughly 18 % of primary energy, in the United States in 2018 (US EIA, 2018). Work towards a goal of achieving net zero energy use buildings will require substantial reductions in the energy consumption within the commercial sector. One proposed step towards attaining this goal is the use of intelligent agents for controlling heating, ventilation, and air conditioning (HVAC) systems used in commercial buildings. An intelligent agent is an autonomous entity that acquires information about the state of the system, makes an optimal or near-optimal control decision, and communicates that decision to another agent or to an actuator that executes the decision. Kelly and

Bushby at the National Institute of Standards and Technology (NIST) completed a feasibility study to determine if intelligent agent technology could lead to significant reductions in HVAC energy consumption. The results of this study demonstrated intelligent agents could produce a cost savings of 21 % over the course of a day (Kelly, 2012).
To further test this concept, NIST created the Intelligent Building Agents Laboratory (IBAL) (Pertzborn,2016-2018). The laboratory is comprised of an HVAC system that emulates a small office building in terms of the complexity and the type of HVAC systems and equipment that would typically be present. It has an air side and water side; the water side contains the plant equipment (e.g., chillers) and the air side, which is the focus of this work, is shown in Figure 1. The airflow path begins with an Outdoor Air Unit (OAU) that emulates outdoor air conditions for the downstream system by preconditioning the actual outdoor air by use of a cooling coil, an electric heating coil, and a steam spray humidifier. After the air is preconditioned in the OAU, it flows into the two Air Handling Units (AHUs). Each AHU is composed of a preheat coil, a cooling coil, and a fan, all in series as shown in Figure 2. The air exiting each AHU flows to two Variable Air Volume (VAV) boxes. The VAV boxes are each composed of a damper blade and a reheat coil in series. Each VAV box delivers supply air to a single zone. The zone simulator includes an electric heater and a steam spray humidifier to emulate the sensible and latent loads of an occupied space. Upon leaving the zone simulators, a portion of the return air stream combines and mixes with the emulated "outdoor air" from the OAU, while the remainder exhausts outdoors. This project considers the various components that condition and control air being delivered to the zones, shown in Figure 2.

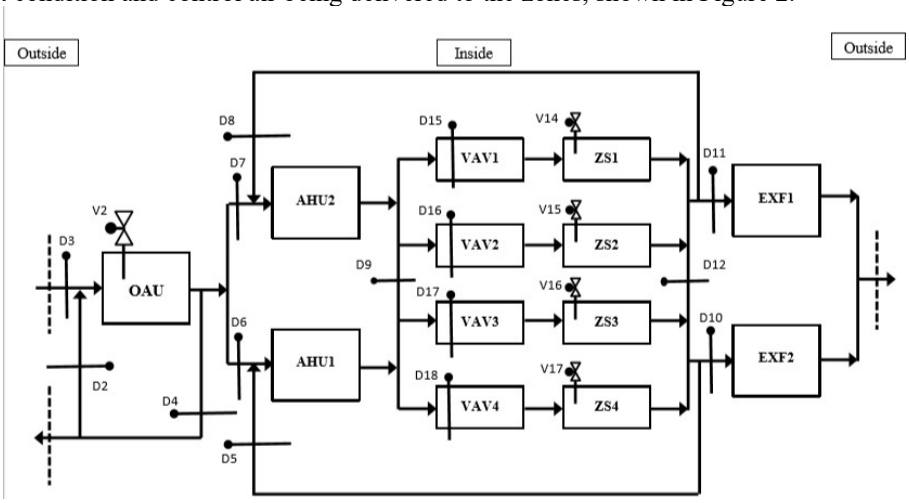

Figure 1: The IBAL Schematic (Pertzborn, 2018)

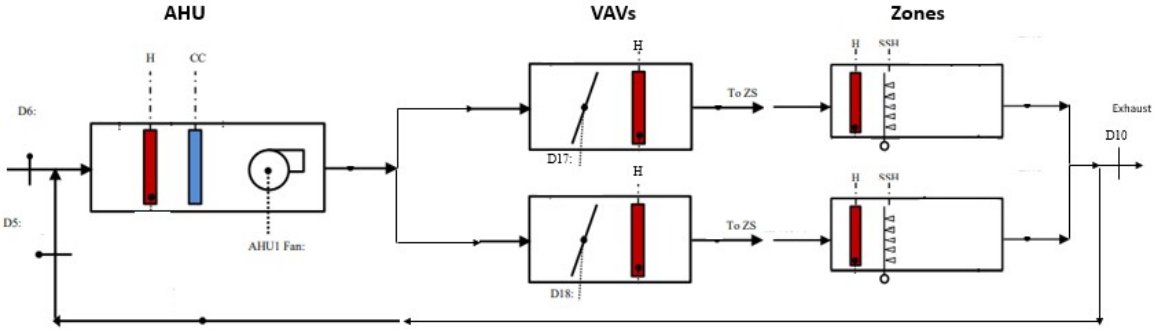

Figure 2: The HVAC system that is being controlled (CC = cooling coil, H = heater, and SSH = steam spray humidifier) (Pertzborn, 2018)

2. COMPONENTS

The simulation modelling focuses on the AHUs and VAV boxes. Each AHU is comprised of an electric heating coil, cooling coil, and draw-thru fan. The electric heating coil preheats mixed air to avoid freezing the glycol mixture flowing through the cooling coil. The cooling coil can provide both sensible and latent heat removal from the supply air stream. Finally, the fan ensures that sufficient airflow is provided to the rest of the system. The VAV boxes include a damper to adjust the flow of the air to the zone and a reheat coil to sensibly heat the air before

delivery to the zone if required. The models developed in the context of this project differ in three ways from previously developed models of VAV air handlers. First, rather than treating the air handler as a whole, models are written for each component (heater, cooling coil, damper, etc.). Second, the models are not load based but are instead designed to compute air and water outlet conditions knowing only the inlet conditions and actuator settings. Third, they need to be able to predict behavior at a small time scale (on the order of seconds) and so are not quasi steady state models, but instead treat the transient behavior of each component.

2.1 Electric Heater

The electric heater model requires two parameters: heater thermal capacitance (C_h) and overall heat conductance (UA). The model also receives operating condition inputs including mass flow ($\dot{m}$), air temperature (T_{in}), relative humidity (RH_{in}), and heater electric power ($\dot{q}_{elec}$).

An energy balance on the heating coil provides:

$$C_h \frac{dT_h}{dt} = \dot{q}_{elec} - \dot{q}_{out} \tag{1}$$

where $\dot{q}_{out}$ is the heat transfer rate from the coil to the air as given by:

$$\dot{q}_{out} = \varepsilon\ \dot{m}\ c\left(T_h - T_{in}\right) \tag{2}$$

where c is the specific heat capacity of air. The parameter, T_h, is the instantaneous coil temperature and ε is the heating coil effectiveness:

$$\varepsilon = 1 - \exp\left(-\frac{UA}{\dot{m}\,c}\right) \tag{3}$$

The differential equation (1) is solved analytically during each time step. The outlet temperature of the air leaving the coil is given by:

$$T_{out} = T_{in} + \varepsilon\left(T_h - T_{in}\right) \tag{4}$$

The parameters C_h and UA are determined through a "calibration" process that involves tuning the model to match experimental data from the IBAL as it operates over a range of conditions. A number of tests were carried out to accomplish this tuning process including ones in which both airflow rate and heating coil power input are varied with time. In total, four tests were used with approximately 2 000 data points per test. An example of one of these tests is shown in Figure 3. Figure 4 shows the measured temperature rise as a function of predicted temperature rise for all the tests considered and indicates that the model can predict the behavior of the coil to within approximately 1 °C under most conditions. The VAV reheat coil uses the same model and the agreement with data from the IBAL system is similar after tuning the parameters.

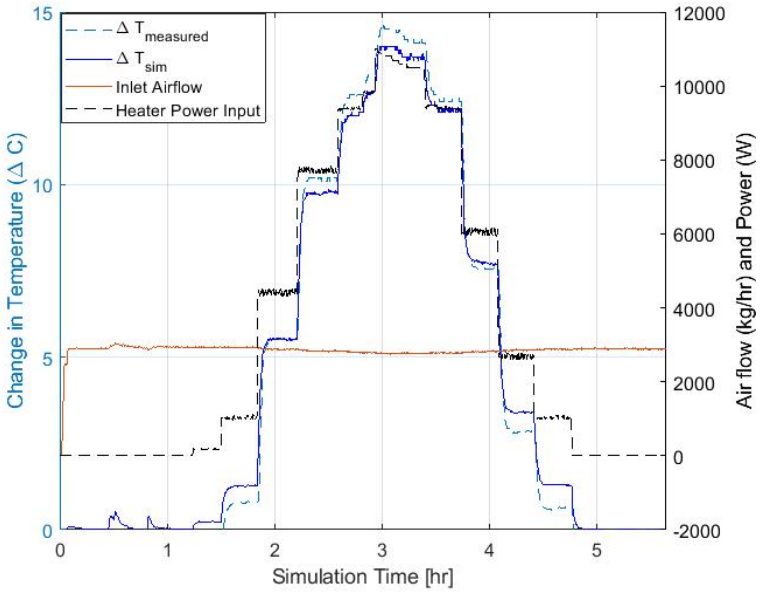

Figure 3: AHU Heater Test Case with Varying Heater Power Input

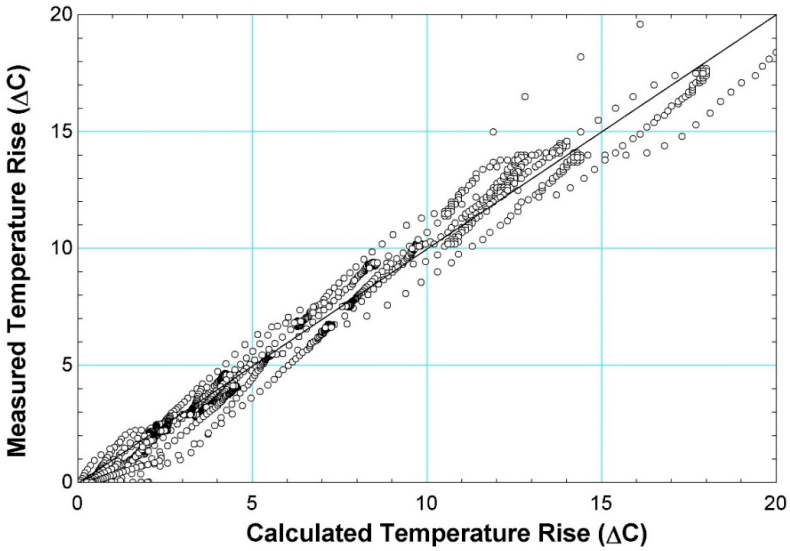

Figure 4: Compiled AHU Heater Data Compared to Simulated Model Output

2.2 Cooling Coil

Figure 5 shows a schematic of a "bypass model" (Stanke, 2000) used as the basis for simulating the cooling coil. The parameters required by this model include the cooling coil capacitance (C_c), the coolant-side conductance (UA_{coil}), and the air bypass fraction (ϕ). The model also requires, as inputs, the inlet air temperature, relative humidity, and air mass flow rate ($T_{a,in}$, RH_{in}, and $\dot{m}_a$, respectively) as well as the inlet secondary fluid temperature and mass flow rate ($T_{liquid,in}$ and $\dot{m}_{liquid}$, respectively).

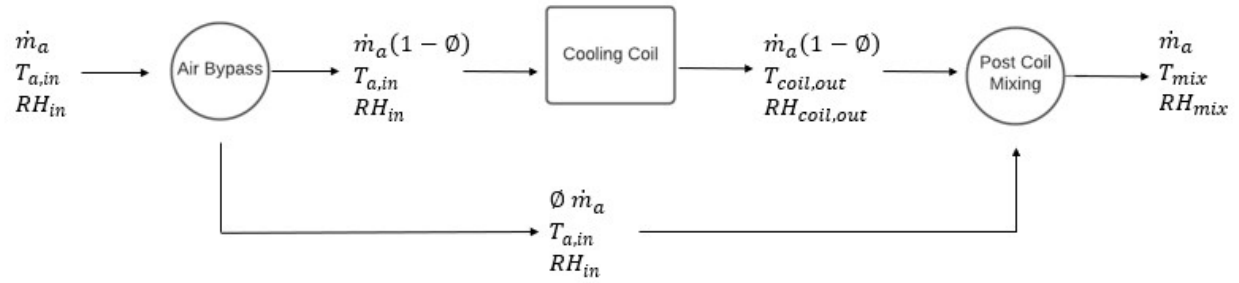

Figure 5: Schematic of the air side of the Cooling Coil bypass model

An energy balance on the cooling coil becomes:

$$\frac{dT_c}{dt} C_c = \dot{q}_{air} - \dot{q}_{liquid} \tag{5}$$

where the rate of heat transfer to the coolant is given by:

$$\dot{q}_{liquid} = \dot{m}_{liquid}\ c_{liquid}\ \varepsilon_{coolant} \left(T_c - T_{liquid,in} \right) \tag{6}$$

where $\varepsilon_{coolant}$ is the effectiveness of the cooling coil based on the coolant side flow:

$$\varepsilon_{coolant} = 1 - \exp\left(- \frac{UA_{coil}}{\dot{m}_{liquid}\ c_{liquid}} \right) \tag{7}$$

The rate of heat transfer from the air is given by:

$$\dot{q}_{air} = \dot{m}_a \left(1-\phi\right) \left(h_{air,in} - h_{coil,out} \right) \tag{8}$$

where $h_{air,in}$ and $h_{coil,out}$ are the moist-air specific enthalpies of the air entering the cooling coil and leaving the cooling coil, respectively. The bypass model assumes that a fraction of the entering air, ϕ, bypasses the cooling coil and the remaining fraction of entering air, (1-ϕ), passes over the cooling coil and leaves the cooling coil at the cooling coil temperature, T_c. If this temperature is below the dew point temperature, then the air is saturated and some condensation has occurred. If the cooling coil temperature is above the entering air dew point temperature, then the air's humidity ratio is unchanged and no condensation occurs.

Within each time step, the simulation numerically solves the ordinary differential equations (ODEs) associated with these equations using an Euler technique to predict the outlet air conditions and the outlet coolant temperature. The outlet coolant temperature is computed by:

$$T_{liquid,out} = T_{liquid,in} + \varepsilon_{coolant} \left(T_c - T_{liquid,in} \right) \tag{9}$$

The bypass airflow mixes with the coil airflow and leaves the coil at temperature T_{mix} and relative humidity RH_{mix}, which are determined by an energy balance and water mass balance on this mixing process.

$$h_{air,mix} = \phi\ h_{air,in} + \left(1-\phi\right) h_{air,out} \tag{10}$$

$$\omega_{air,mix} = \phi\ \omega_{air,in} + \left(1-\phi\right) \omega_{air,out} \tag{11}$$

The parameters C_c, UA_c, and ϕ are tuned to allow the model to predict the behavior of the cooling coil installed in the IBAL. Figure 6 illustrates the results of one test where the coolant flow is varied over time and the predicted vs measured air-side temperature change compared.

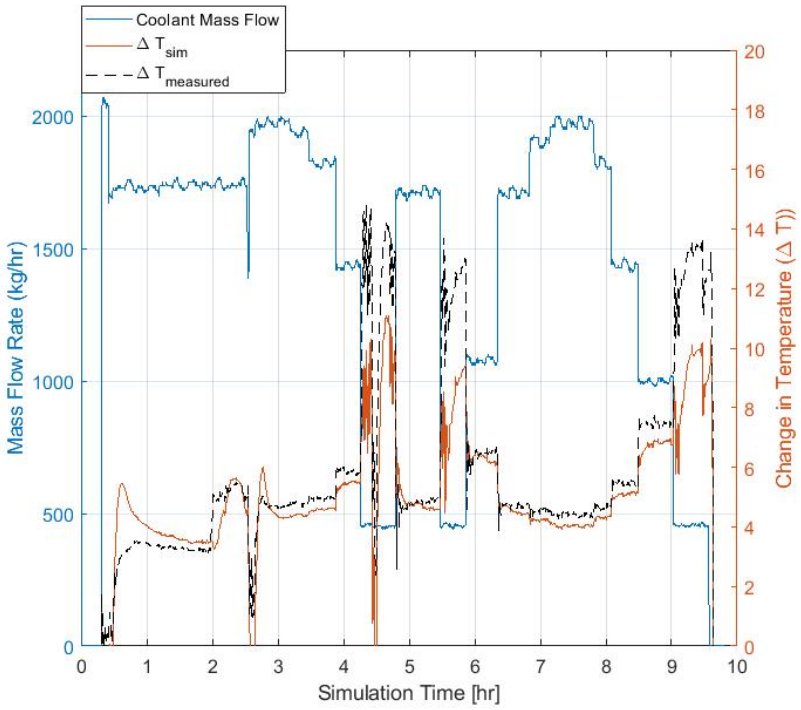

Figure 6: Cooling Coil model validation

Figure 6 shows that the model tracks the data under periods of high coolant flow, but has difficulty predicting the performance when there is extremely low coolant flow (essentially zero volumetric flow). This is an issue that might be addressed by modeling the coil conductance as a function of coolant flow.

2.3 Pressure/Flow Component

Two of the primary mechanisms used to control the HVAC operation are the AHU fan speed and the VAV damper position. The damper position is adjusted to maintain an airflow setpoint, which is determined by the difference between the zone temperature and the zone setpoint. The fan speed is adjusted to maintain a static pressure setpoint, which is reset periodically so that the dampers will be more open. The goal is to reduce fan power consumption by matching the fan speed to the airflow demand. The control system senses pressure as one of the monitoring signals. Therefore, it is necessary for the simulation model to predict how air pressure and airflow within the system change over time as the damper positions and fan speed change. This is accomplished in the Pressure/Flow component, which is a single component that simulates the flow and pressure that exists within one AHU serving two VAV/zones with the associated return air branch (D5), as shown in Figure 7. The model only uses the fan and damper curves to calculate pressure; it does not explicitly model the pressure drop across individual components such as a cooling coil.

The Pressure/Flow component requires the characteristics of the dampers and fans as inputs; these include fan curves (pressure rise vs flow) over a range of speeds and damper resistance curves (pressure drop vs flow) over a range of damper positions. The fan model was derived from the fan curve data provided by the manufacturer for the installed fans. The fan curves were normalized by the maximum pressure rise and maximum flow for each speed (189, 283, 377) rad/s ((1800, 2700, and 3600) rpm) to create the curve fit shown in Figure 8(a). The damper model is obtained from the damper curves provided by the manufacturer. The curves for each damper position, expressed as a % of wide open, %WO, were normalized by the maximum pressure rise and maximum flow for each damper position (45, 50, 60, 70, 80, 90) %WO to generate the curve fit shown in Figure 8(b). The pressure/flow component requires inputs of fan speed and position of all dampers as well as the upstream pressure and the downstream air pressures.

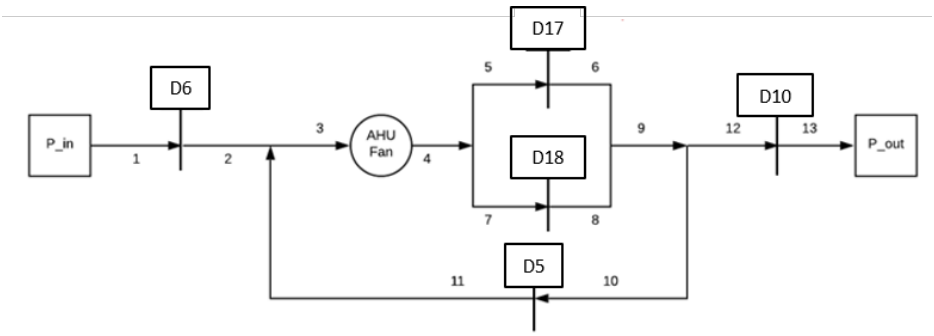

Figure 7: Pressure/flow component, which consists of a single AHU serving two VAV/zone branches and the return air duct. Note that D = damper and the numbered points indicate locations of distinct pressure and/or flow.

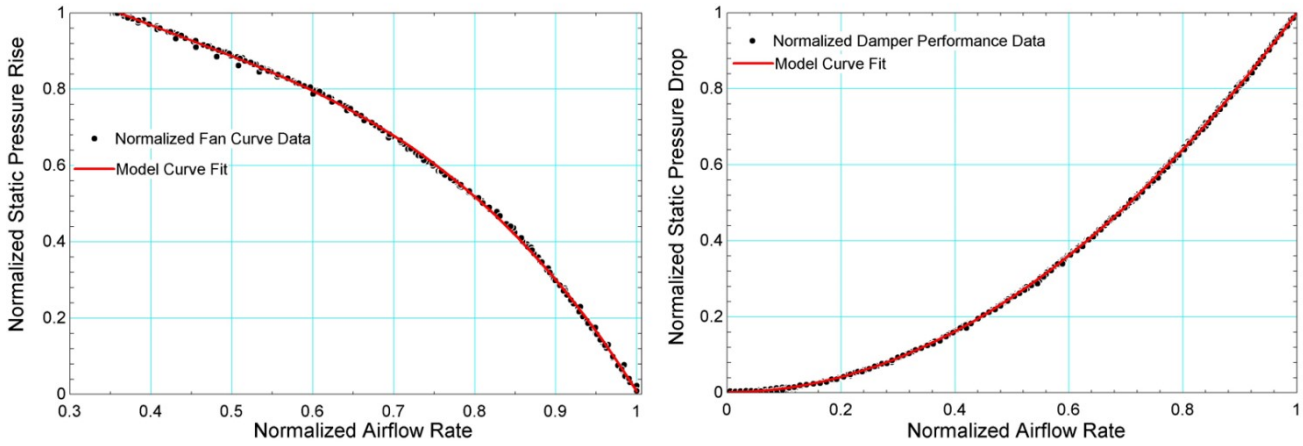

a) b)

Figure 8: a) Normalized fan pressure rise as a function of normalized flow for various fan speeds, also shown is the curve fit used by the model, b) Normalized damper pressure drop as a function of normalized airflow rate for various damper positions, also shown is the curve fit used by the model.

The model enforces continuity of flow and pressure at all nodal intersection points. The process is depicted in Figure 9. At each damper (D), the pressure drop is calculated based on the position of the damper and airflow across the damper. The system is assumed to respond instantaneously for the time scales of interest to changes in fan speed or damper position. The values of flow at node 1 and node 11 are varied until the pressure error terms are negligible, which indicates convergence. To verify the model is working correctly, a few test conditions were simulated. Figure 10 shows the pressures and flow rates at two locations (nodes 4 and 11 in Figure 7) for a case where all damper positions are held constant while the fan speed increases from 189 rad/s (1800 rpm) to 377 rad/s (3600 rpm). Referring to Figure 7, locations 4 and 11 correspond to the location downstream of the AHU fan and the return air branch downstream of Damper 2. Note that downstream of the AHU (at node 4), both the flow and pressure increase quickly as the fan speed increases. The flow and pressure at location 11 are also affected by this change in fan speed; the pressure goes down slightly and the flow increases. The future work associated with this component involves tuning its function to match data from the IBAL.

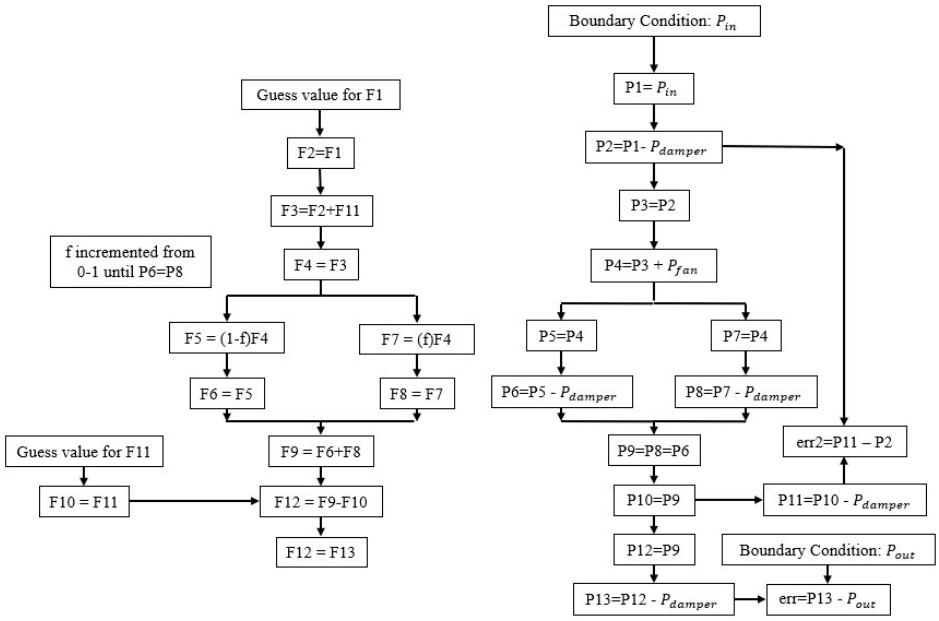

Figure 9: Airflow calculation flow chart

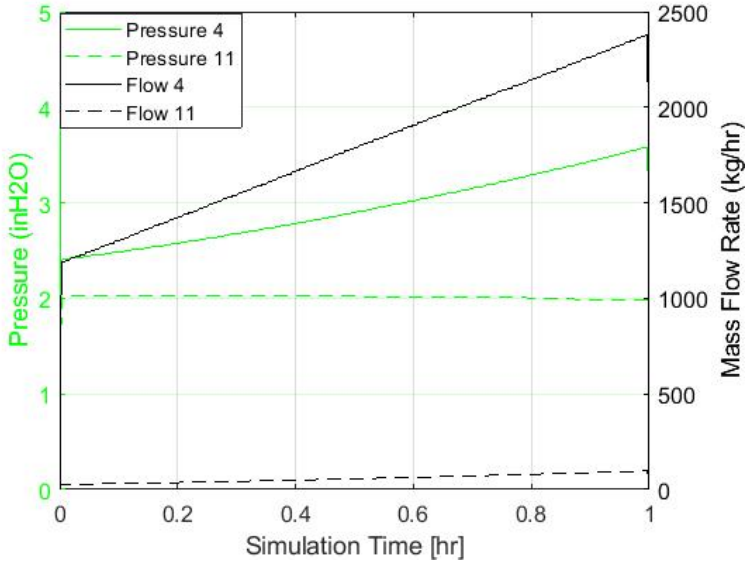

Figure 10: Pressure and flow rate downstream of the AHU (location 4) and in the return branch (location 11) as the fan speed increases.

3. CONTROLLERS

The IBAL simulation model discussed in this paper is flexible with regard to the control system. One of the primary purposes for developing a model is to allow for the simulation of a variety of advanced control strategies prior to deploying them in the IBAL. Initial demonstrations of control function were carried out using a conventional approach that consists of three separate controllers. The first controller is responsible for adjusting the damper in the VAV boxes and activating the reheat coil based on a comparison of the zone temperature to its setpoint. The second controller is responsible for adjusting the fan speed to maintain a setpoint pressure in the supply air duct downstream of the fan and upstream of the VAVs. The final controller is responsible for adjusting the coolant flow through the cooling coil based on the difference between the temperature of the air downstream of the cooling coil (supply air temperature) and its setpoint temperature.

The controllers were tested using a single day that was designed to require both heating and cooling logic. Figure 11(a) shows the outside temperature, the zone setpoint temperature, and the simulated temperature of the zone for this day. For this test, the model inputs and setpoints were set to emphasize the behavior of each controller, which means that the system was generally unable to meet the setpoint. This is not a reflection of what would be expected in a real building, but rather a construct for testing the simulated controllers. During the first 8 hours of the test, the outside temperature drives the zone temperature below the setpoint. Over the next 8 hours, the outside temperature rises, which drives the zone temperature above the setpoint temperature. In the final 8 hours, the outside temperature becomes cool again, which drives the zone temperature below the setpoint.

Figure 11(b) shows the behavior of the VAV controller in response to the zone temperature. During the first 8 hours, the damper position is held at the minimum position while the reheat signal is based on the difference between the zone temperature and the setpoint temperature. Over the next 8 hours, the reheat is turned off as heating is no longer needed. Instead, the controller actuates the damper to open based on the difference in the temperature of the zone compared to the setpoint. In the final 8 hours, the controller reverts to reheat mode. Figure 11(c) displays the cooling coil controller response. Over the first 8 hours and final 8 hours, the mass flow through the coil is at its lowest value because cooling is not needed. In the middle of the simulation, the mass flow increases in response to the rising air temperature downstream of the coil. Figure 11(d) highlights the response of the fan controller. The fan speed remains constant when the damper position is at its minimum value. As the damper opens in the middle portion of the test, the pressure within the system drops, causing the fan speed to increase, which provides a larger volume of cool air during the timeframe when the zone temperature is above the setpoint.

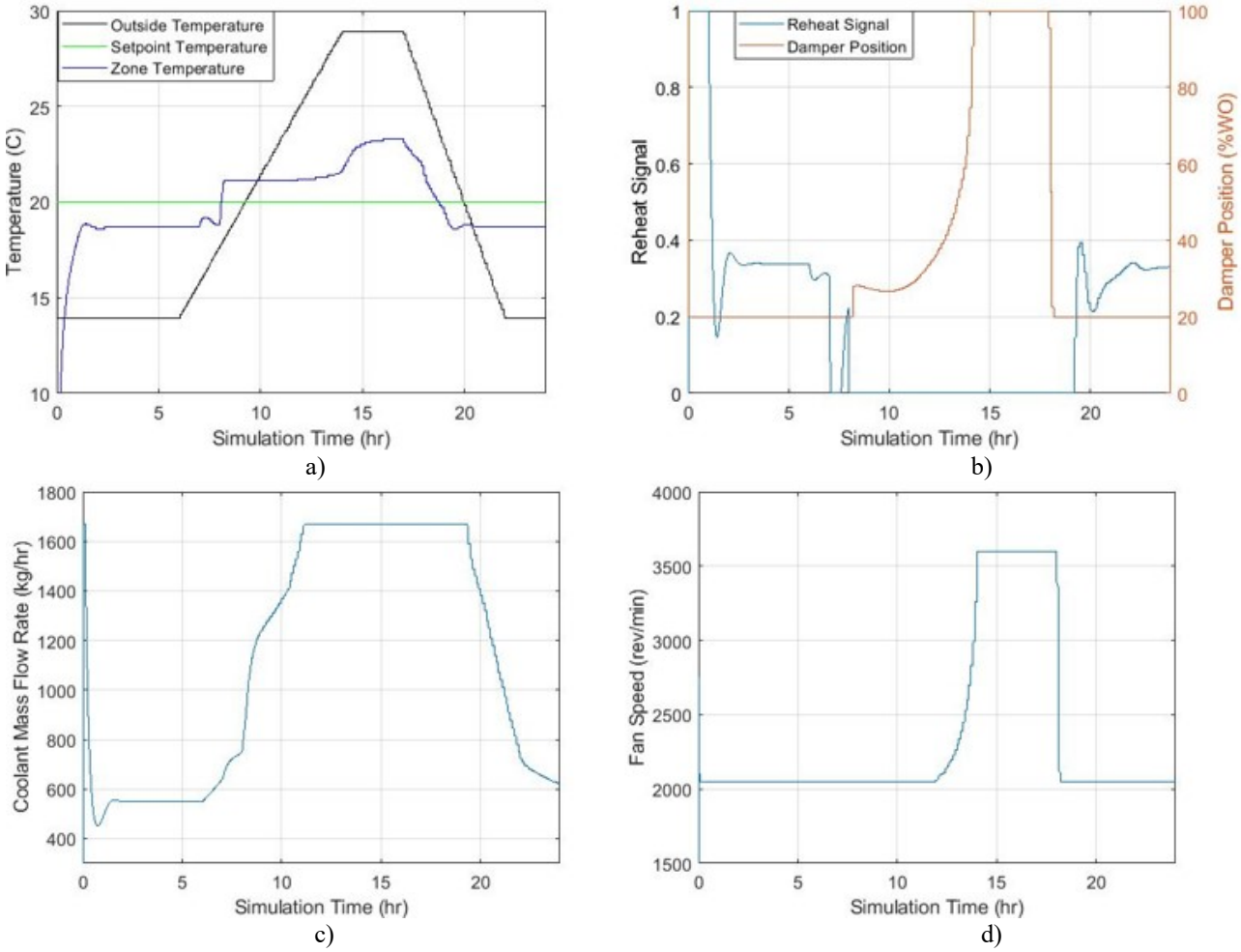

Figure 11: a) Outside air and zone temperature as a function of time, also shown is the zone setpoint temperature, b) VAV controller response including damper position and reheat signal, c) Cooling coil controller response showing coolant flow rate, and d) Fan controller response showing fan speed.

4. CONCLUSION

Once all components have been tuned and validated, the simulation model can be used to test arbitrary controller architectures quickly. The program is designed so that NIST can change between different control strategies seamlessly. One of the proposed control strategies is the use of variable setpoint temperatures throughout the system. This proposed method of control involves the use of predicted weather data to adjust the setpoint temperatures to the various controllers to provide a more optimal control that reduces energy use.

REFERENCES

Kelly, G. & Bushby, S. (2012). Are intelligent agents the key to optimizing building HVAC system performance? *HVAC R Res*., *18*(4), 750–759.

Klein, S.A. et al. (2020). *TRNSYS* (v18) [A Transient Simulation Program]. WI Solar Energy Laboratory, University of Wisconsin.

Pertzborn, A. J. (2016). *Intelligent Building Agents Laboratory: Hydronic System Design* (NIST Technical Note 1933). National Institute of Standards and Technology.

Pertzborn, A. J. (2017). *Measurement Uncertainty in the Hydronic System in the IBAL* (NIST Technical Note 1970). National Institute of Standards and Technology.

Pertzborn, A. J. & Veronica D. A. (2018). *Intelligent Building Agents Laboratory: Air System Design* (NIST Technical Note 2025). National Institute of Standards and Technology.

Stanke, D. (2000). Dehumidify with Constant-Volume Systems: It May Take More than You Think. *Trane Engineers Newsletter*, *29*(4), 4-5.

US Energy Information Administration. (2018). *U.S. energy flow*. https://www.eia.gov/totalenergy/data/monthly/pdf/flow/total_energy.pdf

ACKNOWLEDGEMENT

This research would not be possible without the grant funded by NIST (NIST Award # 70NANB18H203).